



EUROPEAN ORGANIZATION FOR NUCLEAR RESEARCH

CERN-EP/81-166  
18 December 1981

THE CHEMICAL AND MAGNETIC PROPERTIES OF MUONIC  
FREE RADICALS IN SOLUTIONS OF STYRENE IN BENZENE

S.F.J. Cox<sup>\*)</sup>, A. Hill and R. De Renzi<sup>\*)</sup>

CERN, Geneva, Switzerland

ABSTRACT

Implantation of positive muons in solutions of styrene in benzene creates free radicals which are observed and studied by the muon spin rotation ( $\mu$ SR) technique. Muonium-substituted phenylethyl and cyclohexadienyl radicals are identified, and relative rate constants for their formation deduced from the concentration dependence of the  $\mu$ SR amplitudes. There seems to be an indication from the phases of the phenylethyl signals that the precursor may be diamagnetic. Possible broadening mechanisms of the  $\mu$ SR linewidths are surveyed, and the means of distinguishing them through their different dependences on magnetic field, temperature, and concentration is demonstrated. The linewidth of the muonic phenylethyl radical provides a direct measurement of the rate of dimerization in styrene.

(Submitted to Journal of the Chemical Society: Faraday Transactions I)

---

\*) Permanent address: Rutherford Appleton Laboratory, Oxfordshire, OX11 0QX, UK.

CONTENTS

1. INTRODUCTION
  - 1.1 Muon spin rotation
2. INTERPRETATION OF THE  $\mu$ SR SIGNALS
  - 2.1 Frequencies: assignment of the spectra
  - 2.2 Phases: radical precursors
  - 2.3 Amplitudes: radical yields and diamagnetic fraction
  - 2.4 Linewidths: subsequent evolution of the polarization
3. FORMATION OF THE MUONIC RADICALS
  - 3.1 The  $\mu$ SR amplitudes: competition kinetics
  - 3.2 The  $\mu$ SR phases: duration and mechanism of the radical production
4. MAGNETIC AND CHEMICAL PROPERTIES
  - 4.1 Distribution of hyperfine frequencies
  - 4.2 Coupling to nearby protons
  - 4.3 Spin-lattice relaxation
    - 4.3.1 Modulation of  $g-2$
    - 4.3.2 Spin rotation mechanism
  - 4.4 Chemical reaction
5. CONCLUSION

## 1. INTRODUCTION

We present here some studies of muonic radicals in styrene, in benzene, and in solutions of styrene in benzene up to 50% by volume. Similar to the organic free radicals produced by radiolysis of these compounds,<sup>1)</sup> the muonic radicals are paramagnetic species derived from the styrene or benzene molecules themselves but have a particular hydrogen nucleus replaced by a positive muon ( $\mu^+$ ). They are formed when positive muons are implanted in a sample,<sup>2)</sup> and signals from them, very similar to those obtained by magnetic resonance methods, can be observed by the technique which has become known as muon spin rotation, or  $\mu$ SR. These signals are analysed in this paper for the information they contain on the chemical and magnetic properties of the muonic radicals.

### 1.1 Muon spin rotation

By now,  $\mu$ SR is used extensively in condensed-matter physics<sup>3)</sup> where the muon can also play the role of a light-weight proton:  $m_\mu \approx \frac{1}{9} m_p$ . There can be three different aspects of the results obtained. The muon may be a passive probe of the intrinsic properties of the material, as is the case in magnetic materials. Or its behaviour may be compared to that of implanted  $^1\text{H}$ ,  $^2\text{D}$ , or  $^3\text{T}$ , in order to provide a severe isotope-test of theoretical models, as in diffusion studies. Or there may appear quite novel features which are clearly particular to the interaction of the muon with its environment, as is the case for semiconductors. The present work shows all these aspects, and we are able to present some properties which are particular to the "new" radicals, as well as some measurements of chemical reaction rate -- here the initial stages of polymerization -- which are made possible, but are not otherwise influenced, by the muon's presence.

The success of the  $\mu$ SR method relies chiefly on two circumstances.<sup>2)</sup> The first is the availability of spin-polarized muon beams (our experiments use the CJ1 beam line of the CERN Synchro-cyclotron). These beams may be slowed down, and a proportion of the muons can be stopped in the sample. There is no significant loss of polarization during this "thermalization", whether the muon remains as a

bare  $\mu^+$ , as it does in metals, or whether it acquires an electron to form the muonic analogue of hydrogen, called muonium, as it is able to do in semiconductors and in dielectric liquids or solids.<sup>2)</sup> The second circumstance is that on a convenient time-scale (the lifetime is 2.2  $\mu$ s) the muon decays radioactively, emitting a positron preferentially in the direction of its spin. This asymmetry of the decay positron is observable with simple scintillation detectors, the precession of the muon spins in their local magnetic or hyperfine fields manifesting itself as a modulation of the counting rate in a particular detector. It is these precession signals that are the source of information in these experiments.

## 2. INTERPRETATION OF THE $\mu$ SR SIGNALS

The application of the  $\mu$ SR technique to chemistry and its similarity to magnetic resonance techniques, especially ENDOR, has been reviewed in some detail by Roduner and Fischer.<sup>4)</sup> Our own present work is a particular aspect of a broader survey of the chemistry of muons, muonium, and muonic radicals, which is described in the accompanying paper.<sup>5)</sup> We refer to these two articles for the theoretical basis for the interpretation of the  $\mu$ SR precession signals. Briefly, they are treated in two ways.

Firstly a Fourier transform, which may be performed on-line, produces a frequency spectrum such as that depicted in Figure 1a. The majority of our spectra were recorded at 3 kG; at this field two transitions per radical are expected, as indicated in Figure 1b. To a good approximation the corresponding frequencies are separated by twice the  $\mu^+$  Larmor frequency, and centred on the frequency equivalent to half the isotropic hyperfine coupling. The displacement of the peaks with field therefore determines which peaks form a pair, as well as the value of the hyperfine interaction for that radical. Since the electronic polarization is negligible in radicals at ambient temperature and in fields of a few kilogauss, the apparent difference in intensity of the two styrene peaks must represent an instrumental decrease in sensitivity with frequency. This is quantified in the Appendix. Indeed for benzene, only the lower frequency peak is visible, the upper one lying close to the limit of the spectrometer passband.

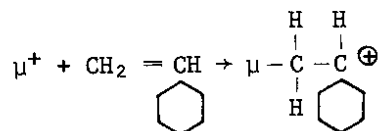
Secondly, an off-line program is able to fit damped waves corresponding to each component, and to determine their respective amplitudes, phases, and decay rates (as well as more precise values for the frequencies). We have used the CERN MINUIT program,<sup>6)</sup> which determines the most likely or best-fit parameter values by minimizing a "chisquare" function. The error bars in our figures represent one standard deviation as determined by the program; our raw precession signals typically represent twenty million muon decays (recorded in two telescopes) and take up to eight hours each to accumulate.

### 2.1 Frequencies: assignment of the spectra

The frequency information (that is, the values of the hyperfine couplings) we use here only in the assignment of the spectra. We observe one radical each in styrene and in benzene and, by comparison with the published hyperfine constants for "normal" or protonic radicals,<sup>1)</sup> identify the species depicted in Table 1. These assignments are justified in the accompanying paper, where we also comment on a small ( $\sim 20\%$ ) discrepancy between the protonic and muonic hyperfine couplings (after scaling for the different magnetic moments,  $m_\mu/m_p \approx 3$ ). This discrepancy, and its decrease with temperature, has been observed in other organic compounds and is the subject of investigation elsewhere.<sup>7)</sup>

### 2.2 Phases: radical precursors

Inspection of the radicals' structure shows that they could be formed, as is usually supposed,<sup>2,7)</sup> by attack of muonium on the appropriate carbon-carbon double bond. We refer to this subsequently as model I. An alternative mechanism, model II, is the direct addition of  $\mu^+$  giving initially the carbonated cation,<sup>7,8)</sup> e.g.



Since this is a diamagnetic species it would then have to very quickly acquire an electron to be observed as the (neutral) radical. A third possibility is that

electrons produced in the track of the slowing muon add first to create styrene (or benzene) anions, the muon then neutralizing one of these -- a process analogous to protonation; however, since the muon may finally stop some distance from the damage it has created, we judge this last mechanism to be the least likely. A clue as to how models I and II may be distinguished appears to be contained in the phases of the  $\mu$ SR signals, which we analyse in subsection 3.2.

### 2.3 Amplitudes: radical yields and diamagnetic fraction

The amplitudes of the fitted waves are measures of the positron asymmetry and therefore of the muon polarization in the particular species [extrapolated to time zero, i.e. approximately (see subsection 3.2) to the moment of creation of the species]. They are therefore proportional to the probability, per muon stopped, that the corresponding species are formed. The absolute values of these probabilities may be determined by comparison of the amplitudes with the amplitude of the  $\mu$ SR signal from a sample of graphite, in which the incoming muon polarization is wholly accounted for in a single line at the Larmor frequency of the free muon. The yields of styrene and benzene radicals presented in Figure 2 are determined in this way. The yield for styrene is the sum of the amplitudes of the lower and higher frequency waves (these are not significantly different after correction for the passband of the spectrometer); that for benzene is taken as twice the amplitude of the observed lower frequency wave. In section 3, the variation of these amplitudes with the concentration of the solution is interpreted in terms of the relative rates of formation of the two radicals, that is of the selectivity of the muonium or muon addition.

In addition to the pairs of lines characteristic of the paramagnetic species, a single line is always seen at the muon Larmor frequency (13.55 MHz/kG). It is supposed (by analogy with protons) that free muons cannot exist chemically in these materials, so this signal is attributed to muons which are in some diamagnetic association with the molecules of the solutions.<sup>2)</sup> The unneutralized muonic carbonium ion, or carbonated cation, invoked above as alternative precursor to the radicals, is one such possibility.<sup>8a)</sup> The nature of the diamagnetic fraction and its

correlation with the electronic properties of the molecules are questions of some interest in muon and muonic chemistry, which we begin to tackle in the accompanying paper.<sup>5)</sup>

#### 2.4 Linewidths: subsequent evolution of the polarization

The damping constants of the fitted waves represent the rates of decay of the muon polarization in the corresponding species. These are decay rates due to processes other than the muon's radioactive decay (which is compensated in the precession signals before their analysis). Exponential decays are assumed in the fitting, so the rates are equivalent to Lorentzian linewidths of the spectral lines. This is appropriate to all the mechanisms of line-broadening which we consider in sections 4 and 5.

It is the determination of the effective mechanisms, by examining above all the qualitative behaviour of the linewidths -- their variation with the parameters concentration, magnetic field, and temperature -- that constitutes the major part of this work.

### 3. FORMATION OF THE MUONIC RADICALS

#### 3.1 The $\mu$ SR amplitudes: competition kinetics

The amplitudes of the styrene and benzene signals are plotted in Figure 2 against the concentration of styrene; they are expressed here as the probability, per muon stopped, that the corresponding radicals are formed. The statistics are good enough to show that these yields do not vary linearly with the concentration but are each functions both of the styrene and of the benzene fraction. If muonium is indeed involved as a precursor, model I, this is a good indication that both components contribute to its production; they then compete for the muonium available in the subsequent formation of their respective radicals, which can be described by simple rate equations:

$$\frac{dR_S}{dt} = k_S M [S] ,$$

$$\frac{dR_B}{dt} = k_B M [B] ,$$

and

$$- \frac{1}{M} \cdot \frac{dM}{dt} = k_S [S] + k_B [B] .$$

Here  $M$ ,  $R_S$ , and  $R_B$  are the probabilities, per muon stopped, of the existence at time  $t$  of a muonium atom or of a styrene or a benzene radical in the sample. The molarities of styrene  $[S]$  and of benzene  $[B]$  are essentially unchanged by the formation of individual radicals, and we suppose that any subsequent reaction of the radicals is much slower than their formation, itself much slower again than the muonium production; integration then gives the final yields to be

$$R_S(t \rightarrow \infty) = \frac{k_S M_0 [S]}{k_S [S] + k_B [B]}$$

and

$$R_B(t \rightarrow \infty) = \frac{k_B M_0 [B]}{k_S [S] + k_B [B]} .$$

Here  $M_0 = M(t = 0)$  is the probability, again per muon stopped, that a muonium atom was formed and remained available for the observed radical formation. Of course similar expressions could hold for the alternative mechanism of radical production with the carbonium ion as precursor, model II;  $k_S$  and  $k_B$  could in that case represent the rate constants for direct muon attachment, and  $M_0$  the proportion of muons that remained available for the purpose. The amplitude information is therefore unable to distinguish between the two models.

The broken curves in Figure 2 represent expressions of this form fitted with a muonium yield (model I) or muon availability (model II), assumed constant,

$$M_0 = 0.35 \pm 0.15$$



and a ratio of the rate constants

$$k_S/k_B = 3.5 \pm 0.15 ,$$

so that the double bond in styrene is more susceptible to attack by muonium (model I) or by muons (model II) than is the benzene ring, by this factor. It is clear that a still better fit can be obtained (particularly for the end points of Figure 2, i.e. for the pure compounds) if the parameter  $M_0$  is greater in benzene than in styrene. Although analogous rate equations can be written for the initial stage of muonium production appropriate to model I, our statistics would not allow their solutions to be included and fitted reliably. The solid curves in Figure 2 represent a purely phenomenological fit with  $M_0$  decreasing linearly with concentration from 0.40 in pure benzene to 0.20 in pure styrene. In fact such a large difference is hardly to be expected for molecules whose electronic properties are so similar; it relies rather heavily on the pure styrene result, however, which may conceivably have been falsified by a degree of polymerization of this sample.

We remark that neither the radical signals, nor the radical signals and the diamagnetic fraction combined, wholly account for the polarization of the incoming muons. Other processes are therefore probably at work which will in any case complicate the set of rate equations and modify their solutions for the observable yields. In styrene, for instance, other muonic radicals are to be expected, corresponding to attack on the phenyl group; their total amplitude will presumably be smaller than that of the principal radical by a factor of the order of  $k_S/k_B$  and will be spread over three frequencies. They cannot therefore be observed with our present statistics but may partially account for the greater "missing fraction" in styrene as compared with benzene.

The magnitude of this problem is illustrated in Figure 3. Since processes contributing to the "missing fraction" may involve either the bare  $\mu^+$  itself or an intermediate stage such as muonium, it is difficult to know how to include them explicitly in the formulation. We demonstrate in subsection 3.2 below that the missing fraction is not simply a question of depolarization of the muons in the

radical precursor; and a careful scrutiny of spectra taken in low fields (10-20 G) does not reveal the presence of a long-lived muonium fraction in these samples.

### 3.2 The $\mu$ SR phases: duration and mechanism of the radical production

If the radicals are formed sufficiently quickly, the frequencies characteristic of their precursor are not detectable in the  $\mu$ SR spectra. They can affect the phases (and amplitudes) of the observed radical signals, however, if the precursor lifetime is not vanishingly small, so that some estimate of this lifetime is sometimes possible. It should even, in principle, be straightforward to distinguish paramagnetic and diamagnetic precursors: the frequencies characteristic of muonium are higher than those of the radicals and the muon Larmor frequency is lower, so they would produce phase shifts of opposite sign.

This can be demonstrated by considering a step change in the Hamiltonian,

$$\mathcal{H} = \mathcal{H}_i \theta(t'-t) + \mathcal{H}_f \theta(t-t'),$$

giving rise to a muon polarization  $P(t, t')$ . The observed amplitudes and phases may then be determined through

$$P(t) = \int_0^{t \gg \tau} \exp(-t'/\tau) P(t, t') dt',$$

$\tau$  being the mean lifetime of the initial stage. A more general approach, with more than two stages, has been worked out by Percival and Fischer,<sup>9)</sup> but the simple version will suffice for our purposes.\*)

---

\*) By way of illustration, for Hamiltonians giving rise to single precession frequencies, the fast reaction limit is characterized by  $\Delta\omega \cdot \tau = (\omega_i - \omega_f)\tau < 1$ . The signal at  $\omega_f$  only is observed in this limit, with its phase shifted relative to its geometrical value (i.e. the value determined by the angular position of the telescope) by  $\Delta\phi = \tan^{-1}(\Delta\omega \cdot \tau)$ , and its amplitude decreased by a factor  $1/\sqrt{1 - (\Delta\omega \cdot \tau)^2}$ .

---

In Figure 4, the phases of the pair of signals from the styrene radical are analysed through their variation with magnetic field. It is convenient to examine first their sum and then their difference to distinguish various contributions to the experimentally measured phases. The chemical phase shift almost vanishes from the sum (Figure 4a), whose nearly linear field dependence allows us to determine the exact origin of time  $t_0$  relative to the beginning of our recorded histograms:

$$\begin{aligned}\phi_{12} + \phi_{34} &\approx 2\phi_0 - (\omega_{34} - \omega_{12})t_0 \\ &\approx 2\phi_0 - 2\omega_{\mu}t_0 .\end{aligned}$$

Here  $\omega_{12}$  and  $\phi_{12}$  are respectively the frequency and phase of the lower frequency transition,  $\omega_{34}$  and  $\phi_{34}$  those of the upper frequency transition in Figure 1b;  $\phi_0$  is the geometrical phase determined by the angular position of the telescope with respect to the incoming beam. The difference then depends on the chemical phase shifts, and therefore on the duration and mechanism of the radical formation:

$$\phi_{12} - \phi_{34} = \Delta\phi_{12} - \Delta\phi_{34} + At_0 .$$

Here the quantity  $At_0$  ( $t_0$  is in principle determined from Figure 3a;  $A$  is the radical hyperfine constant) can be regarded as determining the origin of the grids of theoretical curves shown. The grid for model I lies above, and that for model II below, this origin, which represents a vanishingly small reaction time. It seems as if model I could not be brought into agreement with the data, whereas model II can be fitted with a reaction time  $\tau$  of the order of 1 ns (the corresponding depolarization, or loss of amplitude, is about 20%, approximately constant at all values of the magnetic field employed). It should be mentioned, however, that the determination of  $t_0$  from the phase sum is limited in its precision, and that the phase difference is extremely sensitive to this parameter. So one could slightly force the first fit to bring the data into agreement with model I. Figures 4c and 4d illustrate such an attempt for a muonium lifetime of less than 10 ps (larger times would require an even greater discrepancy in the slope in Figure 4c).

We should await further data before drawing a firm conclusion, but this is a tantalizing indication that the radical precursor may be diamagnetic. For the benzene radical data this sum and difference treatment is not possible; the error bars are anyway too large to allow any interpretation in this case except that they are consistent with reaction times for either model of  $< 1$  ns.

#### 4. MAGNETIC AND CHEMICAL PROPERTIES

The inverse linewidths of the  $\mu$ SR signals are perhaps capable of more direct physical and chemical interpretation than are their amplitudes or phases. These linewidths are presented in Figure 5. To obtain them the precession signals were fitted over time intervals of typically between 2 and 5  $\mu$ s (1000 or 2500 channels at 2 ns per channel). The optimum condition for determining a time constant  $\tau$  is to perform the fit over the interval  $0-2\tau$ , so we expect, after compensation for the radioactive decay, to be able to determine linewidths in the range 0.1-15  $\mu$ s. The results lie comfortably within these limits, and those for styrene, despite the poor precision, show a significant variation with concentration.

We consider below whether these linewidths represent an intrinsic spread in the signal frequency, a process of spin-spin or spin-lattice relaxation, or a chemical inverse lifetime of the radicals themselves. No significant contribution to the linewidth is expected from non-uniformity or instability of the magnetic field: our early measurements (Figures 2 and 5) were made in an iron-cored electromagnet, kindly loaned by the CERN Polarized Target Group, in which the total field variation over the effective sample volume was measured to be less than 250 ppm; later measurements (Figures 6 and 7) were made in a similar magnet shimmed at the Rutherford Appleton Laboratory<sup>10)</sup> to reduce the total variation to below 50 ppm. In each case, locking of the field to a proton NMR gaussmeter<sup>11)</sup> assured a stability in time of better than 50 ppm.

##### 4.1 Distribution of hyperfine frequencies

The hyperfine interaction is written as being isotropic in the Hamiltonian of an individual radical.<sup>4,5)</sup> This anticipates the fact that there will be strong

motional narrowing of any anisotropic component in non-viscous liquids. The narrowing is not "complete", however: if the static anisotropy is of magnitude  $\delta A$ , there will be a residual linewidth<sup>12)</sup> of

$$\lambda_1 \approx \delta A(\delta A \cdot \tau_c) .$$

Here  $\tau_c$  is the correlation time for reorientation of the molecules in the liquid, and the expression is valid in the limit of rapid modulation of the  $\mu$ SR frequency, i.e.  $\delta A \cdot \tau_c \ll 1$ . The variation of the styrene linewidth would then represent some variation of  $\tau_c$  for styrene with the viscosity  $\eta$  of the solution (the bulk viscosities for pure styrene and pure benzene differ by more than a factor of 10, although the relevant local viscosity for a particular species in solution may vary less than this).

This explanation can be discounted, however, on two grounds. An order of magnitude estimate already shows it to be unlikely:  $\tau_c$  calculated for styrene in the Debye model lies in the range 1-10 ps, which is confirmed by Rayleigh scattering measurements.<sup>13)</sup> An unreasonably large anisotropy ( $\delta A \gtrsim 200$  MHz) would therefore be required to explain our linewidths. For this radical, in which the muon is in a  $\beta$  position (i.e. on the carbon atom next to that with the unpaired electron), the anisotropy should on the contrary be proportionately very small.<sup>8b)</sup> More decisive is the temperature dependence of the styrene linewidth, which was measured up to 80°C and is shown in Figure 6. Viscosity, of course, decreases with temperature (approximately by a factor of 2 over this range);  $\tau_c$  should decrease slightly faster,<sup>12)</sup> as  $\eta/T$ , and the linewidth in proportion. In fact the linewidth can be seen to increase significantly.

Since the measured muonic hyperfine interactions are not independent of temperature, some care has to be taken here that gradients or instabilities of the sample temperature do not falsify the linewidth measurements. At the highest temperature of Figure 6 the temperature coefficient of the styrene  $\mu$ SR frequencies is (-) 30 kHz/°C and the variation of our sample temperature not more than a few degrees, so there should be no such artefact. The benzene signal provides a

useful control: although the data are less precise, they are consistent with its linewidth being temperature independent, even though its frequency has a similar temperature coefficient.

The muon is also in the  $\beta$  position in the benzene radical (the hyperfine anisotropy in the analogous "normal" cyclohexadienyl radical is 4% only). In case any decrease in linewidth could be thought to be masked by the temperature artefact, a still more powerful argument in this case concerns the field dependence of the linewidth, and we consider this in the following subsection.

#### 4.2 Coupling to nearby protons

An order of magnitude estimate analogous to that for  $\lambda_1$  also precludes any broadening of the line by dipolar interactions with neighbouring protons. Such local fields would be, at most, equivalent to 100 kHz [a typical value for proton dipolar local fields in organic solids with no molecular motion is 35 kHz;<sup>14</sup>) this has to be corrected for the larger magnetic moment of the muon,  $\mu_\mu/\mu_p \approx 3$ ] and after motional narrowing in the liquid would give a residual linewidth of  $\lesssim 100 \text{ kHz} \cdot (100 \text{ kHz} \cdot 10 \text{ ps})$ , that is, less than 1 Hz. These protons themselves have a hyperfine coupling to the electronic radical, however, which can give rise to splittings of the  $\mu\text{SR}$  lines. This is dealt with formally by Roduner and Fischer.<sup>4</sup>) Their result for a single proton can be used to illustrate the magnitude and field dependence of the effect; the coupling to the single  $\alpha$  proton -- the hydrogen bonded to the carbon atom with the unpaired electronic spin -- will in any case dominate. It is

$$\delta\nu = \frac{A_p}{4} \cdot \frac{A_\mu^2}{(\nu_e + \nu_\mu)^2}$$

where  $A_{p,\mu}$  are the proton and muon hyperfine constants, and  $\nu_{e,\mu}$  are the electron and muon Larmor frequencies proportional to magnetic field. Even if the splitting is not resolved, it will make a contribution to the linewidth which varies as the inverse square of the field,

$$\lambda_2 = \delta\nu \propto H^{-2} ,$$

which is clearly seen for benzene in Figure 7b. A further corroboration (and one which serves to distinguish this from other possible sources of an  $H^{-2}$  field dependence) is that at lower fields this splitting does become resolved. The Fourier transform spectrum obtained off-line for benzene at 1.5 kG is shown in Figure 7c; the separation of the peaks may be seen to correspond to the "linewidth" determined by the computer fit of a single decaying wave.

It is equally clear (Figure 7a) that this is not the explanation of the styrene linewidth. This would be smaller than that for benzene by the cube of the ratio of their respective hyperfine constants [strictly as  $A_p A_\mu^2$  (styrene)/ $A_p A_\mu^2$  (benzene)  $\approx 1/15.6$ ] giving a value at 3 kG not greater than 130 kHz. The observed width is significantly greater, and shows no field dependence.

#### 4.3 Spin-lattice relaxation

A lower limit to the decay rate of the precession signals will always be set by the longitudinal relaxation of the muon polarization. Mechanisms involving interaction with neighbouring nuclei (for instance modulation by the molecular rotation and translation of the muon's dipolar interaction with surrounding protons) will be quite unimportant: in non-viscous liquids at room temperature these will be indistinguishable from the transverse relaxation, with a rate shown in subsection 4.2 to be of the order of 1 Hz. A faster mechanism will be via coupling to the electronic spin of the radical; the electronic spin can be assumed to have its own mechanism of relaxation with a characteristic rate  $1/T_{1e}$  sufficiently rapid to keep it in thermal equilibrium with the liquid "lattice". The admixture of states in Figure 1b then implies<sup>12)</sup> a longitudinal relaxation rate for the muon of

$$\frac{1}{T_{1\mu}} \approx \frac{1}{T_{1e}} \left( \frac{A}{\nu_e} \right)^2 .$$

Even this is unlikely to be important on the  $\mu$ SR time scale. Our observation of two distinct lines per radical puts an upper limit on the possible value of  $1/T_{1e}$ :  $1/T_{1e} \ll A \approx 214$  MHz for styrene, 515 MHz for benzene (otherwise only the average

hyperfine coupling and a single  $\mu$ SR line would be observed). Therefore at 3 kG,  $1/T_{1\mu} \ll 0.13$  MHz for styrene,  $\ll 1.8$  MHz for benzene.

Electronic relaxation would, however, limit the lifetime of our precession signals in a more direct manner. This is a phenomenon which is inherent in the  $\mu$ SR method, and which can be understood as follows. In the high field limit of the Breit-Rabi diagram (Figure 1b) which for argument we take to correspond to our experimental conditions, the muon and electron spins can be regarded as decoupled. In radicals formed with electron "spin-up", for instance, the signal can be thought of as that of muons precessing at the "top" transition frequency  $\nu_{12}$ . If in an individual radical the electron spin flips before the muon decays radioactively, the muon continues to precess at the "bottom" frequency  $\nu_{34}$  but does not contribute to the  $\mu$ SR signal at this frequency since its phase with respect to the incoming muon is lost. The signal at frequency  $\nu_{34}$  comes only from radicals formed initially with the electron "spin-down". The  $\mu$ SR signals will therefore have a contribution to their linewidths equal to the probability per unit time of the electron flips, that is

$$\lambda = 1/2T_{1e} .$$

In contrast to the expression for  $\lambda_1$  this is the limit of slow jumping between two frequencies.<sup>12)</sup>

It is unlikely that there will be any dipolar relaxation<sup>12)</sup> from other electronic spins, since paramagnetic impurities should be absent from our samples. In particular, oxygen was removed by the "freeze-pump-thaw" method, which is considered adequate for ESR work. Other (protonic) free radicals will certainly be produced by radiation damage along the track of the incoming muon. Even if some of these are initially "within range", i.e. close enough to interact magnetically with the muonic radical, they will however disperse on a time scale which is at worst



characterized by simple diffusion, probably  $10^{-10}$ - $10^{-9}$  s in benzene<sup>\*)</sup>. They could be responsible for a small "instantaneous" loss of polarization, but no subsequent relaxation.

---

\*) Of a group of particles implanted at  $t = 0$  in a small volume around  $\underline{r} = 0$ , the fraction to be found per unit volume around the point  $\underline{r}$  at a later time is  $(4\pi Dt)^{3/2} \exp(-r^2/4Dt)$ , i.e. for the present purpose the particles can be considered dispersed over a volume of order  $(4\pi Dt)^{3/2}$ ; the self-diffusion coefficient  $D$  is  $2 \times 10^{-5}$  cm<sup>2</sup>/s for benzene.

---

Therefore, for individual muonic radicals in solution, mechanisms for relaxation of the electron spin must be sought in the Hamiltonian<sup>4,5)</sup> for the single radical. Only terms which are a) modulated by the molecular motion and b) able to flip the electronic spin can be effective; in the following sections we consider those most likely to be important.

#### 4.3.1 Modulation of $g-2$

Any departure of the radical's  $g$ -factor from its free electron value indicates an admixture of excited states with non-zero orbital angular momentum. Orbital momentum implies a certain spatial distribution of electric charge, which is not isotropic. The quantity  $(g-2)$  will therefore be modulated as the molecule tumbles in the liquid, and this is able to induce transitions of the electronic spin since some orbital momentum also implies that the true spin is not identical with the fictitious spin  $S$  used in the Hamiltonian. This is the single spin relaxation mechanism identified for solid paramagnets by Van Vleck,<sup>15)</sup> who demonstrated that the corresponding matrix element  $M$  is directly proportional to  $H$ , the magnetic field. ( $M$  contains two interference terms which have the spin-spin and spin-orbit operators interchanged: one has energy denominator  $\Delta - g\beta H$ ; the other, with the sign of the spin-orbit operator reversed, has a denominator  $\Delta + g\beta H$ ;  $\Delta$  is the separation of the level with orbital momentum. The "Van Vleck cancellation" is therefore complete, and the mechanism ineffective, in zero field.)

The corresponding transition probability is then<sup>12)</sup>

$$1/2T_{1e} = M^2 J(\nu_e) ,$$

where

$$J(\nu_e) = \tau_c / \sqrt{1 + (2\pi\nu_e \tau_c)^2}$$

is the intensity or spectral component of the reorientation of the molecules at the appropriate frequency  $\nu_e = g\beta H/\hbar$ . In the limit of rapid reorientation therefore [which should just correspond to our conditions: we have  $(2\pi\nu_e \tau_c)^2 \sim 1/10$ ] the matrix element is the only source of field dependence in the relaxation rate, and the corresponding contribution to the  $\mu$ SR linewidth varies as

$$\lambda_3 = 1/2T_{1e} \propto H^2 .$$

Temperature and the solute concentration  $[S]$  influence the relaxation rate only through the correlation time  $\tau_c$  for molecular reorientation, so that

$$\lambda_3 \propto \eta/T .$$

It is their different dependences on field, temperature, and concentration which will most readily serve to distinguish the different mechanisms of line broadening, so these dependences are entered in Table 2.

#### 4.3.2 Spin rotation mechanisms

Modulation by the molecular reorientation of the anisotropic hyperfine interactions between the unpaired electron and the muon, or the hydrogen nuclei of the molecule, is another source of relaxation for the electron. The spin operators do not commute with the electronic Zeeman energy, so the matrix element for the transition has the same magnitude  $A_{an}$  as the anisotropic part of the hyperfine constant. The contribution to the linewidth is therefore

$$\lambda_4 \approx A_{an}^2 J(\nu_e) = A_{an}^2 \tau_c .$$

It varies with temperature and styrene concentration again as  $\eta/T$ , but is independent of magnetic field.

Dipolar coupling of the electron to the surrounding protons, both of the same and of neighbouring molecules, will likewise give a contribution which is not distinguishable in form, but is likely to be less important in magnitude. If there should be any other paramagnetic species, their effect can also be included here: Abragam's expression for dipolar relaxation<sup>12)</sup> can be rewritten (to within a numerical factor) as

$$1/T_{1e} \sim \{\gamma^4 \hbar^2 / d^6\} \{Nd^3\} \tau'_c.$$

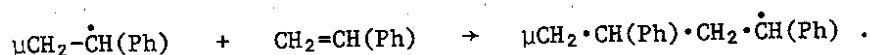
Here the first factor characterizes the maximum strength of the dipolar interaction (the square of the matrix element),  $d$  being the molecular diameter;  $N$  is the density of paramagnetic species so  $Nd^3$  characterizes the proportion of molecules with an electronic spin and is expected to be minute -- this is the quantity which vanishes rapidly as  $(4\pi Dt)^{-3/2}$  if the species are created in the spur;  $\tau'_c$  is now a time characterizing the translational motion, an order of magnitude larger than the rotational correlation time but again varying as  $\eta/T$ .

Since the isotropic hyperfine interaction is the appropriate average value for the lowest vibronic state of the molecule, its modulation by molecular vibrations cannot be invoked as a relaxation mechanism. Molecular collisions (that is transitions between vibronic levels) could in principle make a contribution, but one which (with matrix elements reduced by the factor  $A/v_e$ , and a much smaller characteristic time) is negligible beside  $\lambda_4$ .

Notice that in the opposite limit of slow molecular tumbling,  $J(v_e) \rightarrow 1/\tau_c (2\pi v_e)^2$ , so that the relaxation mechanisms  $\lambda_3$  and  $\lambda_4$  would have the "opposite" temperature dependence, and an additional factor in the inverse square of the field.

#### 4.4 Chemical reaction

Suppose now that the radicals react chemically. For the styrene (phenylethyl) radical this is most likely to be a combination with another monomer molecule; that is, the initial stage of polymerization:



The muon is so far removed from the unpaired electron in the product that its hyperfine interaction is much reduced. In any case its characteristic frequency could not be observed in the  $\mu$ SR spectrum since no phase relation with the initial signal is preserved; muons decaying in the dimer or higher molecules contribute only to the unpolarized background signal.

The rate of disappearance of the monomer radical therefore contributes directly to the decay rate of its  $\mu$ SR signal. We suppose a first-order reaction, so that the contribution has the form

$$\begin{aligned}\lambda_s &= -\frac{1}{R_s} \frac{dR_s}{dt} = k[S] \\ &= A[S] e^{-E_a/kT} .\end{aligned}$$

For the styrene signal the observed concentration dependence and the absence of any field dependence are at least consistent with this; the Arrhenius temperature dependence is unmistakable, however (Figure 6), and serves to distinguish a chemical reaction from the other mechanisms of  $\mu$ SR line-broadening entered in Table 2. From the usual semi-logarithmic plot (Figure 6b), we obtain values which are not unreasonable for polymerization:<sup>16)</sup>

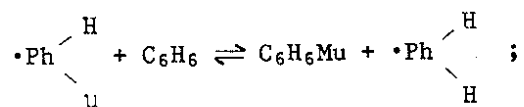
$$E_a = 8.0 \pm 2.5 \text{ kcal/mole}$$

for the activation energy, and

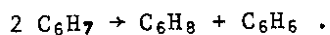
$$\ln A (1 \cdot \text{mole}^{-1} \cdot \text{s}^{-1}) = 25 \pm 3$$

for the pre-exponential factor. These values are modified slightly (towards the upper error limits) if a reasonable residual linewidth is first subtracted.

For the muonic benzene (cyclohexadienyl) radical, no such rapid chemical reaction is expected, but there are other possibilities.<sup>8b)</sup> One is intramolecular transfer, in which the proton adjacent to the muon moves one position around the ring and the muon, left alone, folds down into the plane of the ring. This would substantially reduce the hyperfine coupling. Alternatively, internuclear transfer of hydrogen would leave the muon in a diamagnetic state:



(the analogous intermolecular transfer of muonium would introduce the unpaired electron to a new set of ring protons with a different instantaneous spin configuration, thus broadening the  $\mu\text{SR}$  line, but not by an amount of any significance here). The rate constants for these processes will be relatively low however<sup>15)</sup> (lower still for the styrene radical, the methyl group being much less reactive). The eventual fate of the cyclohexadienyl radical is uncertain, unless it can encounter other radicals produced in the spur:



The absence of a strong temperature or concentration dependence of the linewidth of the benzene  $\mu\text{SR}$  signal is therefore no surprise. It dismisses chemical reaction as a broadening mechanism for benzene, whose  $\mu\text{SR}$  linewidth is successfully accounted for (subsection 4.2 and Table 2) by proton hyperfine coupling.

## 5. CONCLUSION

Muonium-substituted phenylethyl and cyclohexadienyl radicals (Table 1) have been identified and studied by the muon spin rotation technique. The spectra are simpler than those usually obtained by magnetic resonance methods and do not require, for their observation, concentrations of the species so high that magnetic interactions or relaxation may obscure their chemical interpretation. These are two advantageous consequences of the extreme dilution of the muon probe; the modest statistics of the results displayed here are limited only by our present counting rates.

Rate constants for the formation of the radicals have been deduced from the amplitudes of the  $\mu\text{SR}$  signals, and in particular from their variation with the concentration of styrene in solution in benzene. If muonium is the precursor, as is usually supposed, these rate constants measure the selectivity of its attack on the olefinic bond and phenyl ring in these compounds. The effective yield of muonium in these solutions can also be deduced and, from the phase of the signals,

its maximum lifetime estimated. The preliminary indication from the phases of our phenylethyl signal that its precursor may in fact be diamagnetic, probably in that case the muonic carbonium ion, is however sufficiently provocative to deserve further investigation.

As far as a study of the fundamentals of muon and muonium chemistry is concerned, styrene and benzene are perhaps not a well-chosen combination, the electronic properties of their molecules being too similar, but we indicate in the accompanying article<sup>5)</sup> how progress may be made in this field. The structures of the two radical molecules are quite different at the respective points of attachment of the muon, however, so the similarity of the isotope effect in the two cases is a coincidence of some interest.<sup>5)</sup> The information on molecular conformation and dynamics contained in muonic hyperfine constants, and especially in their variation with temperature, is already being exploited elsewhere.<sup>7)</sup>

Consideration of the possible mechanisms of broadening of the  $\mu$ SR spectral lines shows how these can be identified, often uniquely, by their dependence on such parameters as concentration, temperature, and magnetic field. This is illustrated in Table 2, which summarizes the possibilities appropriate to our materials and experimental conditions. The observed qualitative behaviour (also entered in the table), supported by order of magnitude estimates, dismisses broadening by spin-spin or spin-lattice processes in these samples. For the cyclohexadienyl radical the linewidth is characterized by a strong field dependence and is accounted for by the hyperfine coupling of the  $\beta$  proton.

The identification for the muonic phenylethyl radical is particularly interesting: the concentration and temperature dependences suggest strongly that its  $\mu$ SR linewidth represents a chemical reaction rate. It can be assumed that the muon, although influencing to some extent the conformation of the methyl group which it labels, does not significantly affect the reactivity of the radical, so this is a direct measurement of the rate of dimerisation of styrene.

These results for two particular compounds serve also, we hope, to illustrate the extent of the information that is available from the  $\mu$ SR method.

Acknowledgements

We are indebted to G. Allen (SERC) and G. Stirling (RAL) who proposed the  $\mu$ SR study of monomer solutions<sup>5)</sup> and have followed the progress of the work with interest. The advice of M.C.R. Symons (University of Leicester) on the chemical aspects (subsections 2.2 and 4.4) has been invaluable.<sup>6)</sup> Our preliminary results were presented at the ETH Zurich  $\mu$ SR Meeting, 10-11 September 1981; we wish to thank those present for their comments, especially H. Fischer and E. Roduner, (University of Zurich), who also kindly sent us a preprint of their related work prior to publication,<sup>7)</sup> and P.W.F. Lowrier (NIKHEF) for his suggestions regarding the competition kinetics, subsection 3.1.

We also wish to record our thanks to the Parma, Uppsala and CERN  $\mu$ SR groups for their general support with the experimental work.

REFERENCES

- 1a) C.H. Bamford and C.F.H. Tipper (eds.), *Comprehensive chemical kinetics* (American Elsevier Scientific Publ. Co., Inc., NY, 1975), Vol. 14.
- 1b) K. Eiben and R.H. Schuler, *J. Chem. Phys.* (1975) 62, 3093.
- 2a) J.H. Brewer, K.M. Crowe, F.N. Gygax and A. Schenck, *in* *Muon Physics*, Vol. III: *Chemistry and solids*, eds. V.W. Hughes and C.S. Wu (Academic Press Inc., NY, 1975), p.3.
- 2b) A. Schenck *in* *Exotic atoms*, eds. G. Fiorentini and G. Torelli (Servizio Documentazione dei Laboratori Nazionali di Frascati, Italy, 1977), p. 335.
- 2c) J.H. Brewer and K.M. Crowe (Benzene radical reference), *Ann. Rev. Nucl. Part. Sci.* (1978) 28, 239.
- 3a) F.N. Gygax, W. Kündig and P.F. Meier (eds.), *Proc. First Int. Topical Meeting on Muon Spin Rotation*, Rorschach, Switzerland, 1978 (North-Holland Publ. Co., Amsterdam, 1979).
- 3b) J.H. Brewer and P.W. Percival (eds.) *Proc. Second Int. Topical Meeting on Muon Spin Rotation*, Vancouver (BC), Canada, 1980 (North-Holland Publ. Co., Amsterdam, 1981).
- 4) E. Roduner and H. Fischer, *Chem. Phys.* (1981) 54, 261.
- 5) A. Hill, G. Allen, G. Stirling and M.C.R. Symons,  $\mu^+$ SR studies of organic liquids. Accompanying this article.
- 6) F. James and M. Ross, *Comput. Phys. Commun.* (1975) 10, 343.
- 7) E. Roduner, W. Strub, P. Burkhard, J. Hochmann, P.W. Percival, H. Fischer, M. Ramos and B.C. Webster, Muonium-substituted organic free radicals in liquids. Muon-electron hyperfine coupling constants of alkyl and allyl radicals, Submitted to *J. Chem. Phys.*
- 8a) M.C.R. Symons, Private communication, July 1981.
- 8b) M.C.R. Symons, Private communication, November 1981.



- 9) P.W. Percival and H. Fischer, Chem. Phys. (1976) 16, 89.
- 10) G.P. Warner, Rutherford Appleton Laboratory preprint RL-81-083 (1981).
- 11) K. Borer and G. Fremont, preprint CERN-EP/77-19 (1977).
- 12) A. Abragam, The principles of nuclear magnetism (Clarendon Press, Oxford, 1961).
- 13) G.R. Alms, G.D. Patterson and J.R. Stevens, J. Chem. Phys. (1979) 70, 2145.
- 14) S.F.J. Cox, S.F.J. Read and W. Th. Wenckebach, J. Phys. C. (Solid State Physics) (1977) 10, 2917.
- 15) J.H. Van Vleck, Phys. Rev. (1940) 57, 426.
- 16) P.J. Flory, Principles of polymer chemistry (Cornell University Press, Ithaca, NY, 1953).

Table 1

Muonic radicals identified

Radical formed	Hyperfine interaction constant measured at various temperatures
Styrene $\rightarrow$ muonic cyclohexadienyl $\text{CH}_2 = \underset{\text{C}_6\text{H}_5}{\text{CH}} \rightarrow \mu - \underset{\text{H}}{\overset{\text{H}}{\text{C}}} - \underset{\text{H}}{\overset{\text{H}}{\text{C}}}\cdot$	A(25 °C) = 212.4 $\pm$ 0.02 MHz (15.8 G) A(40 °C) = 209.9 $\pm$ 0.06 MHz A(60 °C) = 207.3 $\pm$ 0.03 MHz A(80 °C) = 205.7 $\pm$ 0.1 MHz
Benzene $\rightarrow$ muonic phenylethyl $\text{C}_6\text{H}_6 \rightarrow \text{C}_6\text{H}_5 - \overset{\mu}{\underset{\text{H}}{\text{C}}}$	A(25 °C) = 512.2 $\pm$ 0.1 MHz (38 G) A(40 °C) = 510.4 $\pm$ 0.08 MHz A(60 °C) = 509.1 $\pm$ 0.1 MHz

The ambient temperature values are in reasonable agreement with those measured elsewhere.<sup>2c,7)</sup>

Table 2

Qualitative behaviour of the  $\mu$ SR linewidths.

Mechanism  $\lambda_2$  is identified for the benzene (cyclohexadienyl) radical,  $\lambda_5$  for the styrene (phenylethyl) radical

Broadening Mechanism	Reference in Text	Concentration Dependence	Field Dependence	Temperature Dependence
Intrinsic width: Anisotropic hyperfine Proton hyperfine	(Section)			
	$\lambda_1$ 4.1	As $n([S])$	$H^0$	As $n(T)/T$
	$\lambda_2$ 4.2	$[S]^0$	$H^{-2}$	$T^0$
Electronic relaxation: Modulation of (g-2) Spin rotation	$\lambda_3$ 4.3.1	As $n([S])$	$H^2$	As $n(T)/T$
	$\lambda_4$ 4.3.2	As $n([S])$	$H^0$	As $n(T)/T$
Chemical reaction	$\lambda_5$ 5	$[S]^1$	H	$\exp(-E_A/kT)$
Observed variation: Benzene radical Styrene radical	Figures { 5, 6 & 7	Approx indept. Increase approx as $[S]$	Decrease as $H^{-2}$ Approx indept. Doubles every 20 °C	Approx indept.

Appendix

CALCULATION OF THE SPECTROMETER PASSBAND

A time-to-digital converter (TDC) is used in our experimental apparatus to measure the time interval between the incoming muon and the outgoing positron signals. The main limitation on our frequency resolution results from the sampling performed by this TDC. Given a certain time resolution of the clock,  $\tau$ , we can express the measured time intervals as

$$t = \tau(\ell + x)$$

with  $\ell$  an integer and  $0 \leq x < 1$ .

The oscillator that drives the clock is continuously running so that these time intervals will be seen by the TDC completely at random with respect to its internal beats ("asynchronous" averaging). Thus the probability for a time  $t$  to be measured in channel  $\ell_0$  will be (see Figures 7a and 7b):

$$p(t_1, \ell_0) = p[\tau(\ell+x), \ell_0] = (\ell-x)\delta_{\ell, \ell_0} + x\delta_{\ell, \ell_0-1}$$

If now we consider a wave signal  $A \cos \omega t = A \cos \omega\tau(\ell+x)$ , the content of the  $\ell^{\text{th}}$  channel will be given by

$$y_{\ell_0} = A \sum_{\ell} \int_0^1 dx p[\tau(\ell+x), \ell_0] \cos \omega\tau(\ell+x) .$$

By substituting the proposed probability function, one can evaluate the integral to obtain

$$y_{\ell_0} = A \left( \frac{2}{\omega\tau} \right)^2 \sin^2 \frac{\omega\tau}{2} \cos \omega\tau\ell_0 = AF(\omega\tau) \cos \omega\tau\ell_0 ,$$

where we define  $F(x)$  as our passband function. The behaviour of  $F(x)$  is shown in Figure 7c. Let us suppose that  $\tau = 2$  ns, for the sake of argument. One can see that the first zero of the passband function occurs at  $\omega/2\pi = 500$  MHz ( $x=1$ ). However, the highest frequency directly visible is that of period  $2\tau$ , i.e.  $\omega/2\pi = 250$  MHz. This means that also a frequency  $250 < \omega/2\pi < 500$  MHz is detectable, but it will appear as a lower one. To see how it will show up, one has to substitute:

$$\omega\tau = 2\pi - \theta \quad (0 < \theta < \pi) ,$$

which gives:

$$y_{\lambda} = AF(\omega\tau) \cos (\theta\lambda + \phi_0) .$$

This is just equivalent to the complement to 500 MHz of the original frequency, the phase being reversed. In practice  $F(\frac{1}{2})$  is already equal to 40%, so that, for instance, a 250 MHz frequency will appear in a Fourier power spectrum with 16% of its original height.

Furthermore, our calculation constitutes just the main contribution to the actual passband: a second limitation, whose dependence on  $\omega$  is not easily computed, stems from the time jitter of our signals. A qualitative analysis of its nature, together with an estimate of its upper limit ( $\pm 0.3$  ns), shows that its effect will be negligible in the lower part of our spectrum, but it will further cut down the power of our "duplicated" spectrum ( $250 < \omega/2\pi < 500$  MHz), thus bringing it in most cases below the noise level.

Figure captions

- Figure 1 The  $\mu$ SR spectrum (a) of a 0.5 molar solution of styrene in benzene and the corresponding transitions on the Breit-Rabi diagram (b) for a single radical. The spectrum was recorded at 3 kG and at ambient temperature, and its  $\mu^+$  peak (the diamagnetic signal) at 40 MHz has been suppressed.
- Figure 2 Concentration dependence of the amplitudes of the styrene ( $\bullet$ ) and benzene ( $\blacktriangle$ ) muonic radicals. The curves show the fitted solutions of rate equations for the radical formation assuming a constant (broken lines) and diminishing (solid lines) precursor yield, as explained in subsection 2.1.
- Figure 3 Concentration dependence of the diamagnetic and of the paramagnetic signal amplitudes. The diamagnetic fraction is the amplitude of the signal at the  $\mu^+$  Larmor frequency; the paramagnetic fraction is the total amplitude of the observed radical signals, phenylethyl plus cyclohexadienyl.
- Figure 4 Phase-shift fits for the phenylethyl signal. In (a) the experimental results are fitted with  $t_0 = 8.8$  ns, which determines the position of the theoretical curves in (b) (--- = muonium precursor, -.- = diamagnetic precursor; the numbers represent the chemical lifetime of the precursor in ps). In (c) the fit is forced to  $t_0 = 7.8$  ns, as explained in subsection 2.2; thus the curves in (d) are shifted down by 80 degrees. The signals were recorded at ambient temperature from a 2M styrene solution.
- Figure 5 Concentration dependences of the linewidths of a) the phenylethyl and b) the cyclohexadienyl signals. In (a) a linear increase is drawn, consistent with  $\lambda_5$  and in (b) a constant value, consistent with  $\lambda_2$ .
- Figure 6 Temperature dependence of the phenylethyl linewidth. The fitted decay rates for both the lower frequency transition  $\nu_{12}$  (o) and the upper  $\nu_{34}$  ( $\Delta$ ) are shown (there appears to be some inconsistency for the ambient

temperature measurement). The curve in (a) is the fitted Arrhenius dependence, obtained from the semi-logarithmic plot of the corresponding rate constants (b). The solution was 2M styrene, the field 3 kG.

Figure 7 Field dependences of the linewidths of a) the phenylethyl and b) the cyclohexadienyl signals, and a portion of the frequency spectrum of the cyclohexadienyl signal at 1.5 kG (c). The solid line in (b) is an  $H^{-2}$  dependence; the broken line includes a constant residual linewidth of 100 kHz. The spectra were recorded from a 2M styrene solution at ambient temperature.

Figure 8 The spectrometer passband calculation. (a) and (b) illustrate how the start ( $\mu^+$ ) and stop ( $\beta^+$ ) signals may fall with respect to the clock signal fed to the TDC; the passband function is plotted in (c) against the reduced frequency  $X = \nu\tau$ , where  $\tau$  is the bin width of the TDC.

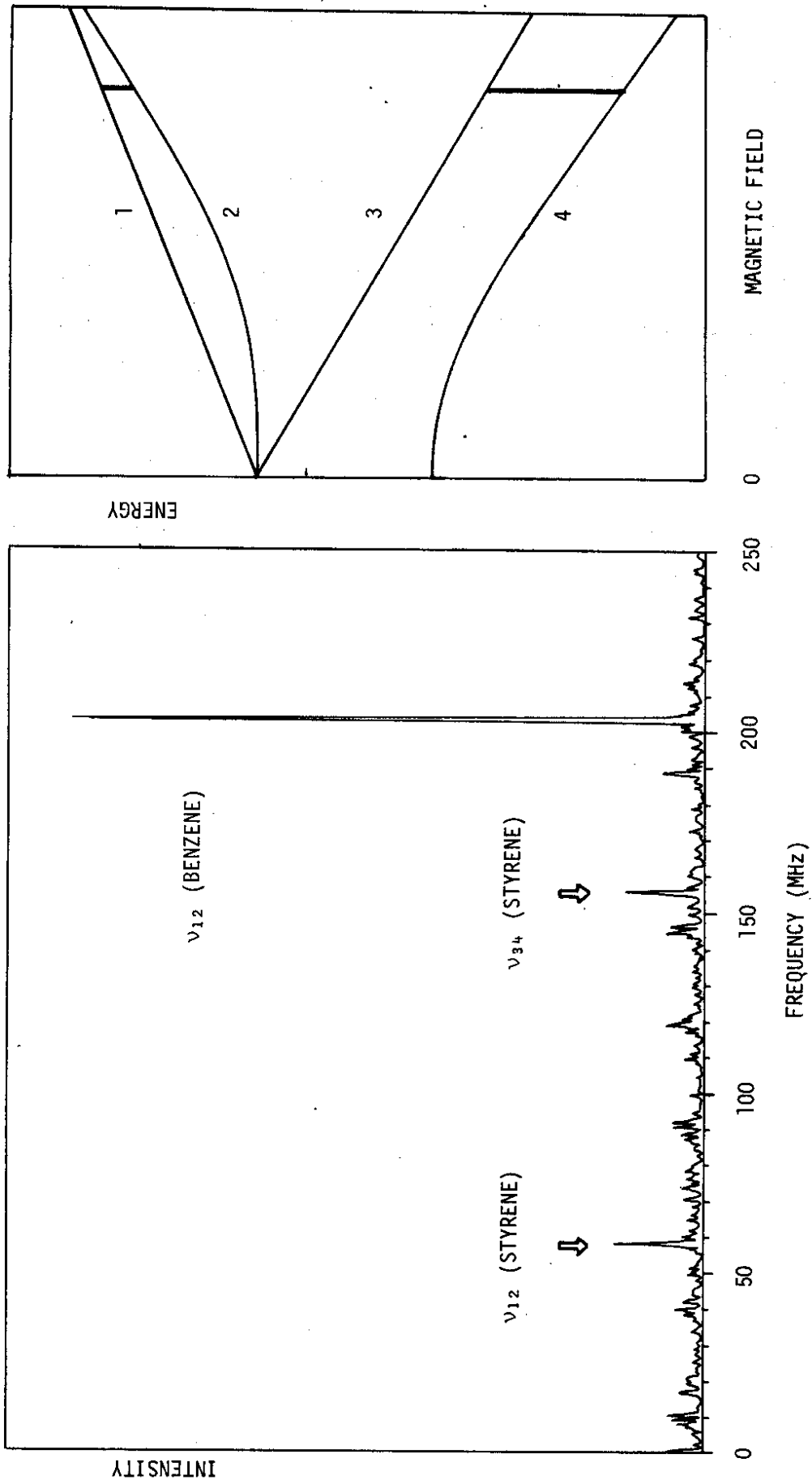


Fig. 1



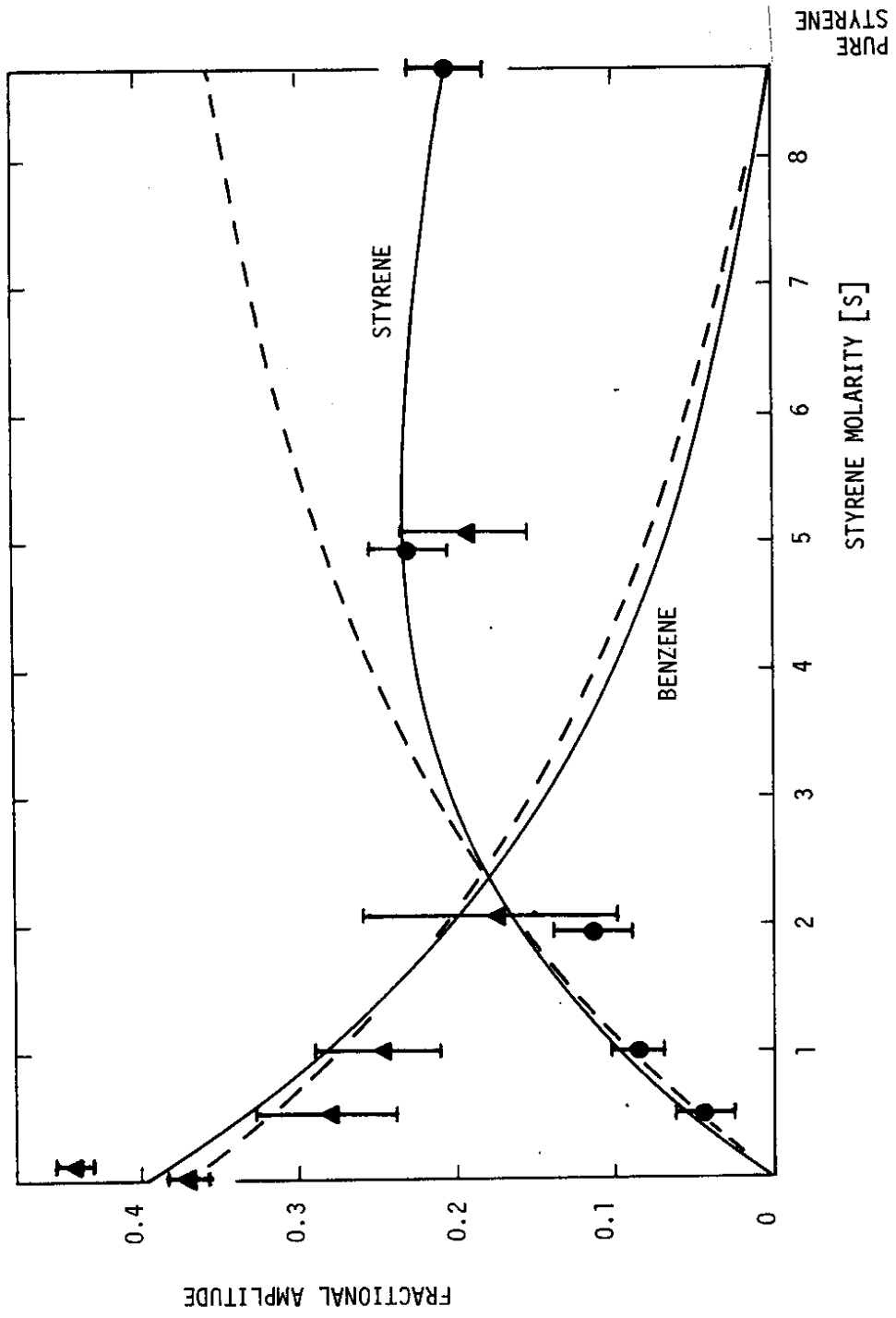


Fig. 2

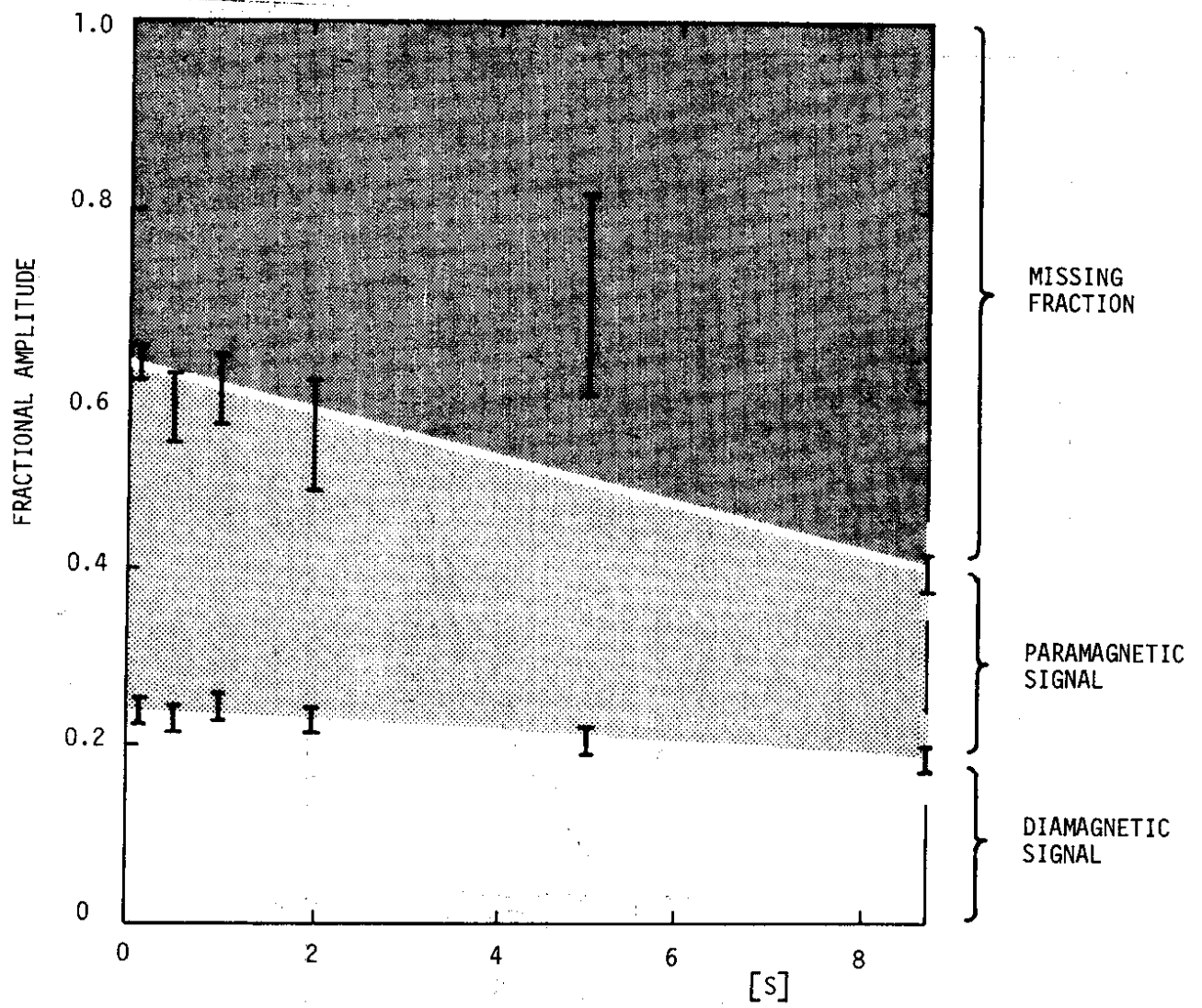


Fig. 3

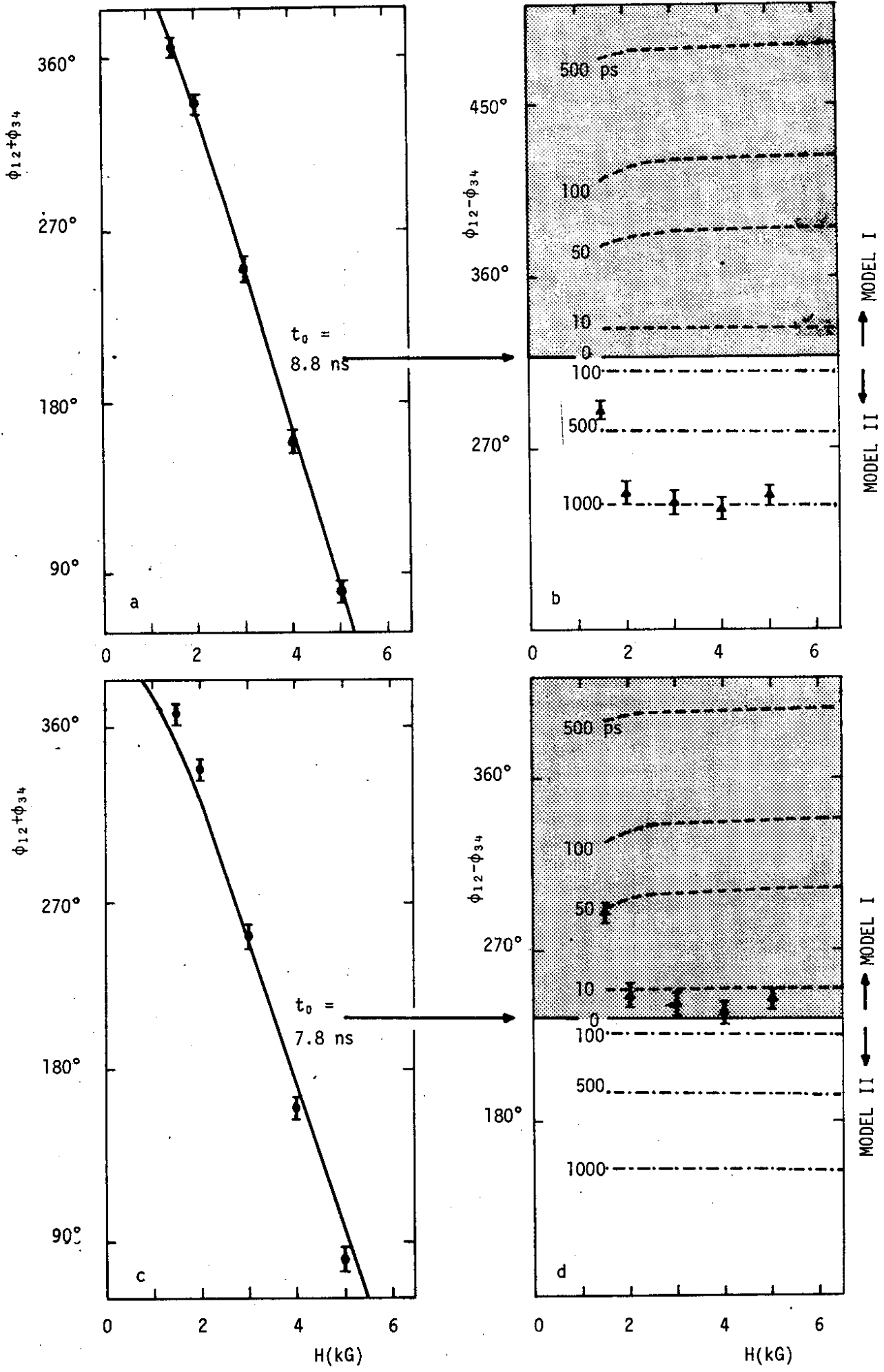


Fig. 4

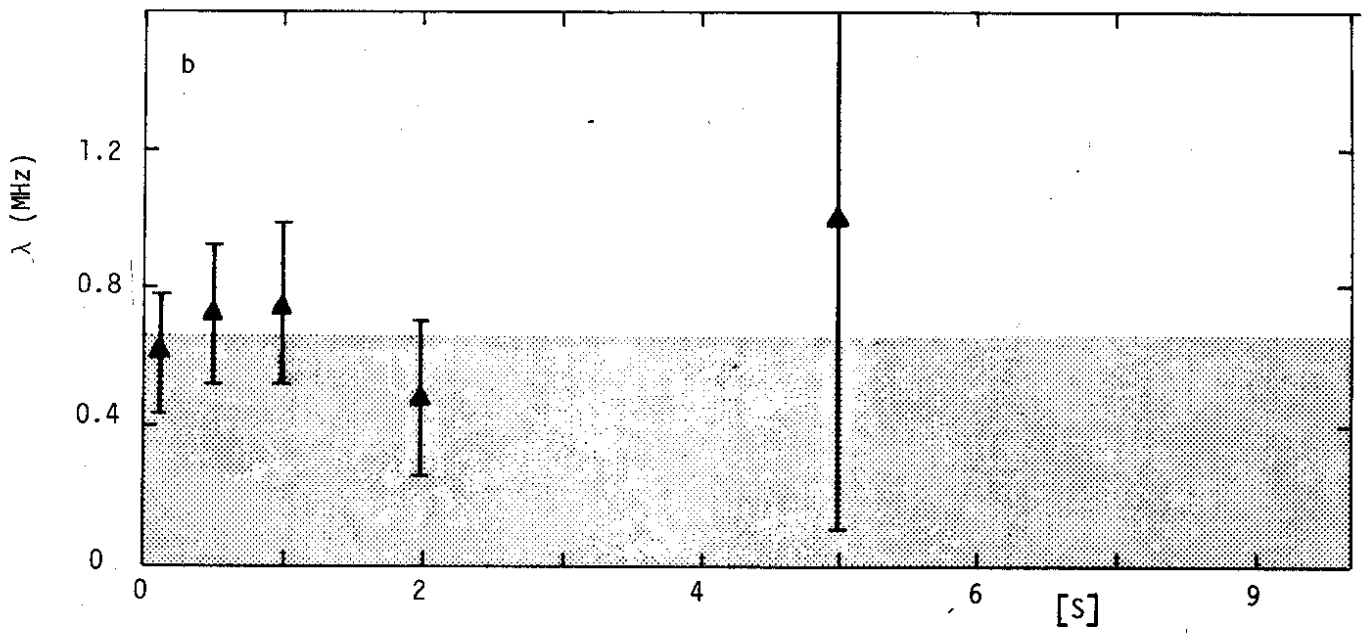
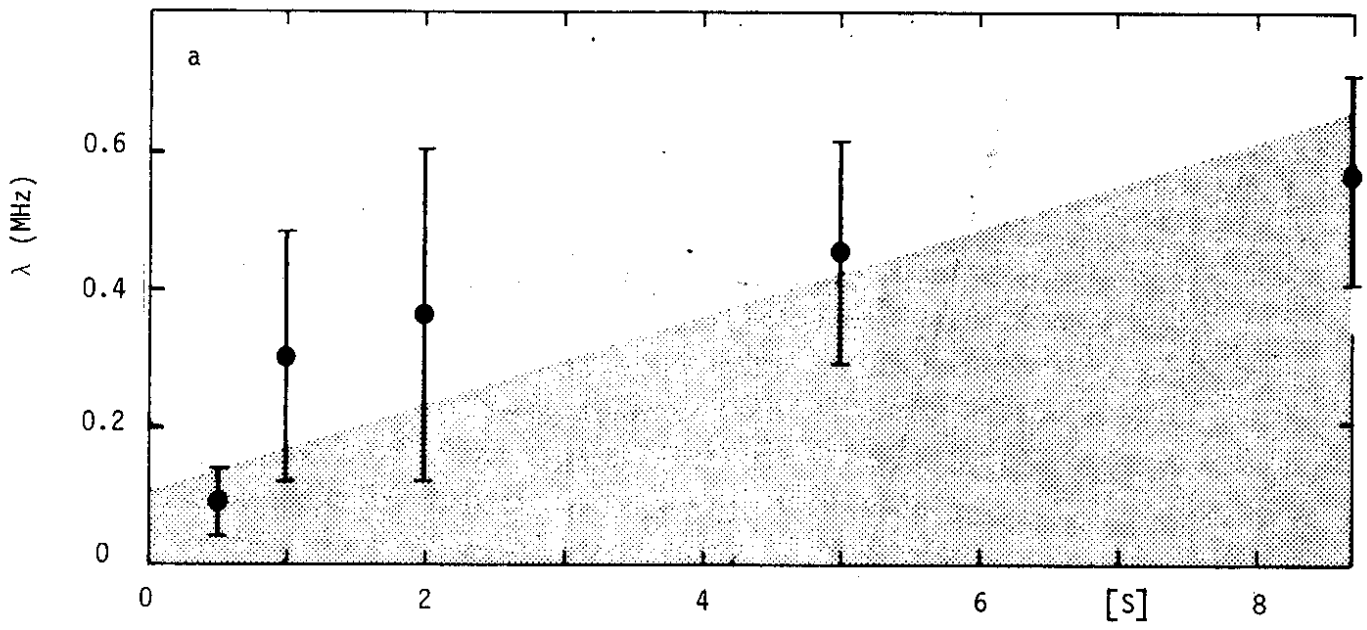


Fig. 5

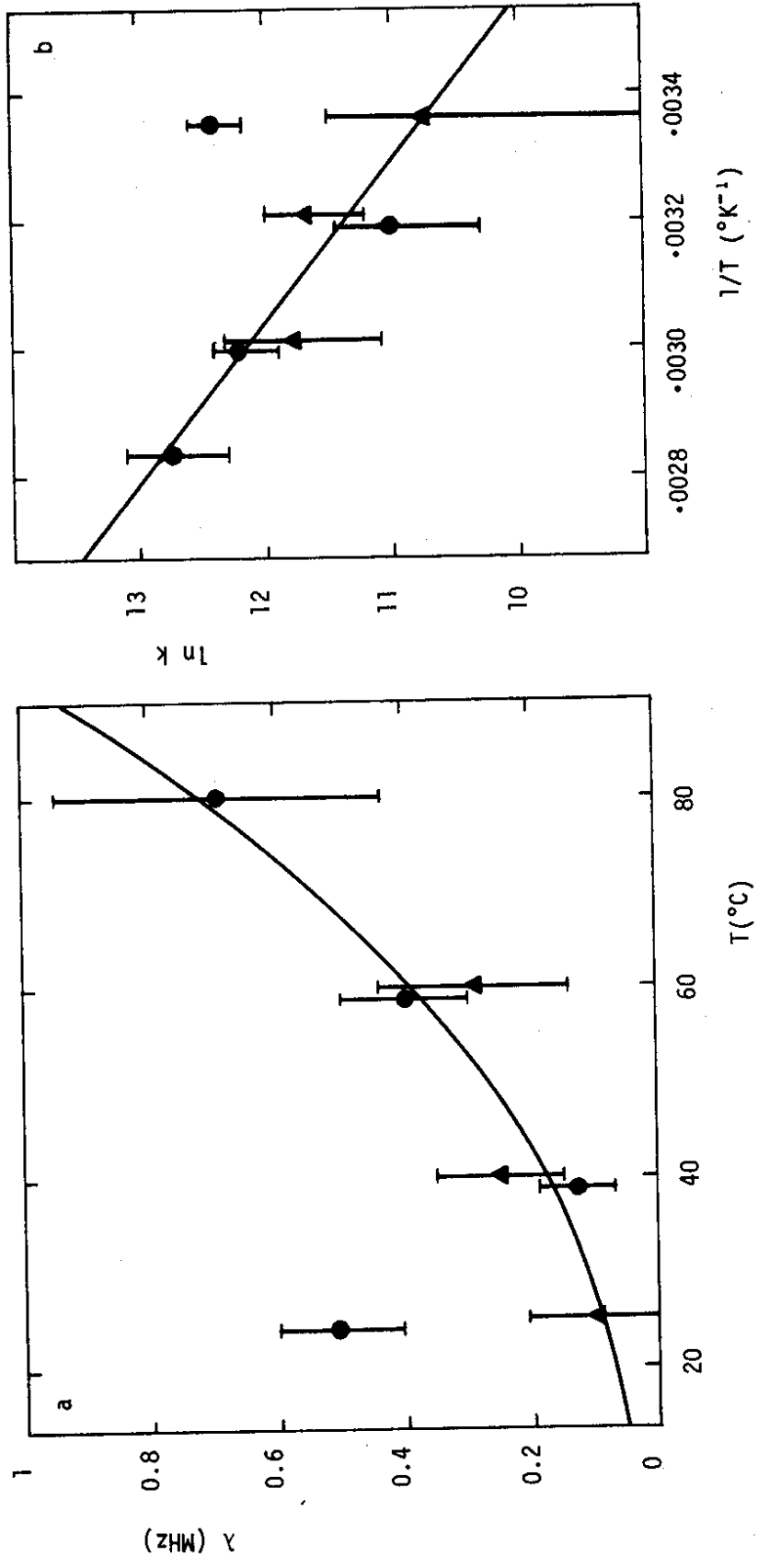


Fig. 6

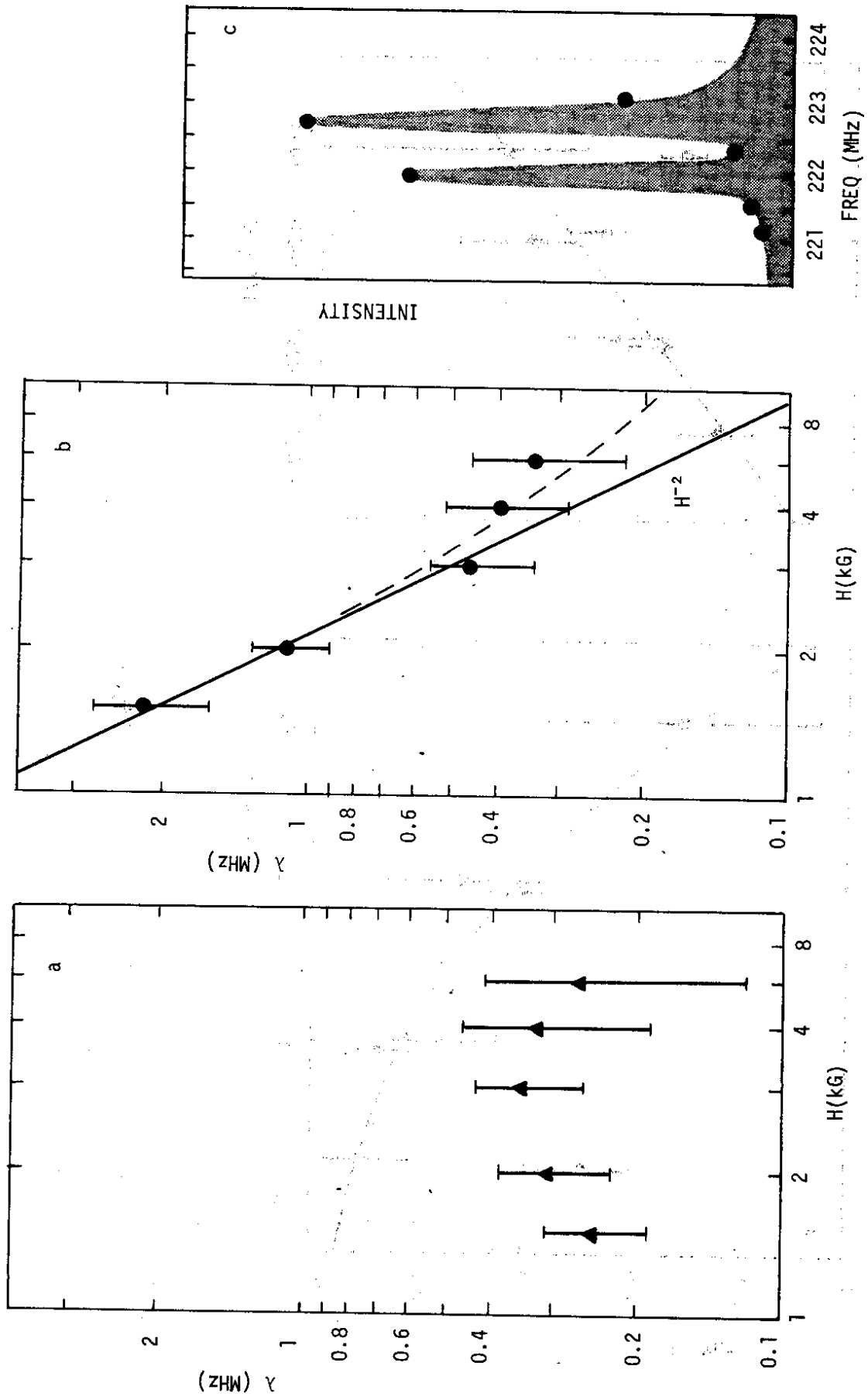


Fig. 7

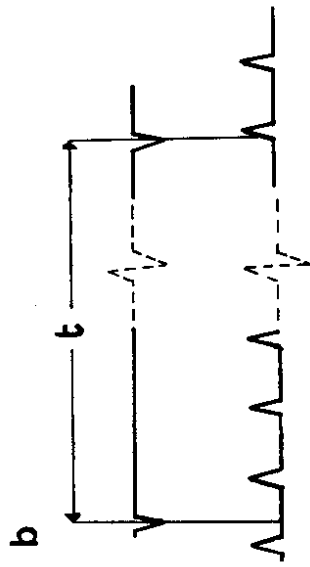
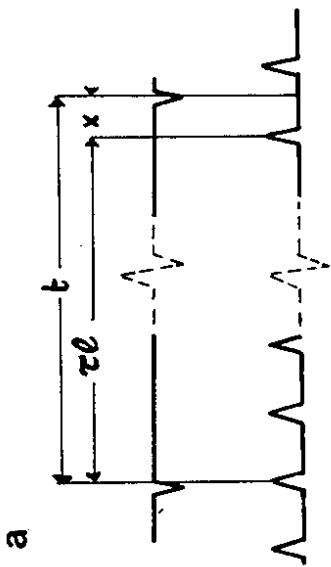
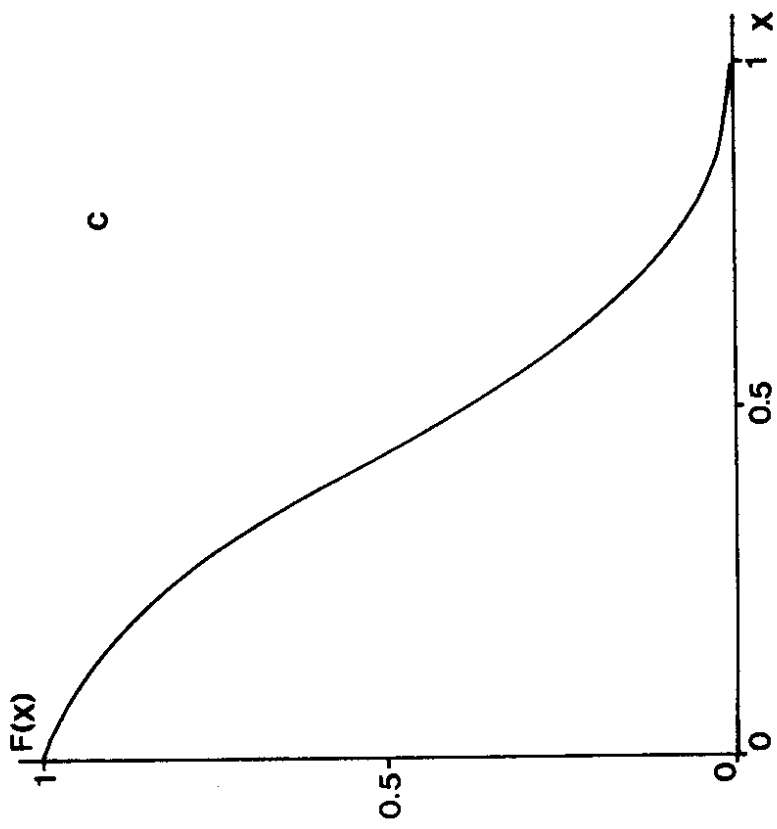


Fig. 8

